Contents lists available at SciVerse ScienceDirect

Tectonophysics

journal homepage: www.elsevier.com/locate/tecto

SKS splitting beneath Alaska: Regional variability and implications for subduction processes at a slab edge

Jenny Hanna, Maureen D. Long *

Department of Geology and Geophysics, Yale University, PO Box 208109, New Haven, CT 06520, USA

ARTICLE INFO

ABSTRACT

Many aspects of subduction zone geodynamics remain poorly understood, including the pattern of flow in the mantle surrounding subducting slabs. Because of the relationship between deformation and seismic anisotropy, measurements of shear wave splitting in subduction zones can shed light on this pattern of flow. While observations of splitting in subduction zones are numerous and robust, the source and geodynamical implications of the anisotropy remain imperfectly constrained. The Alaska subduction zone, associated with the subduction of the Pacific plate beneath North America, is a particularly complex tectonic setting. Dramatic lateral variations in slab morphology, seismicity, and volcanic character are present beneath the region, and previous splitting observations and modeling studies have suggested the possibility of significant along-strike mantle flow in the region. Here we present SKS splitting measurements from more than 50 stations of the permanent broadband AK network located throughout Alaska. Splitting patterns show significant regional variability, but proximate stations often exhibit similar splitting behavior. Stations in southern Alaska exhibit nearly trench-normal fast directions, while in southeasternmost Alaska fast directions trend parallel to the plate boundary. A group of stations in the eastern part of the array exhibit predominantly null splitting, while stations to the northwest of this group tend to exhibit ~1 s or more of splitting with fast directions that are roughly NE–SW. Stations east of the Kenai Peninsula region exhibit complicated splitting patterns that suggest complex anisotropy. We discuss a number of potential factors that may contribute to the complexity in splitting patterns observed in Alaska, including frozen anisotropic structure in the overriding plate lithosphere, asthenospheric shear due to absolute plate motion, trench-parallel flow in the mantle wedge, two-dimensional entrained flow beneath the slab, and mantle upwelling at the slab edge.

© 2012 Elsevier B.V. All rights reserved.

1. Introduction

The pattern of mantle flow in subduction zones remains poorly understood, but is likely substantially more complicated than an idealized two-dimensional model, which invokes corner flow in the mantle wedge above the slab and entrained flow beneath it. This is particularly true in subduction systems with significant complexities, which can include complicated slab morphology, complex overriding plate structure, and the presence of a slab edge. Alaska is an example of such a complicated subduction zone. A simple 2D flow model for Alaska is likely inadequate, but the controls on the three-dimensional pattern of mantle flow beneath Alaska remain poorly understood. Shear wave splitting is an important tool for characterizing mantle flow, and can yield insight into the geometry of seismic anisotropy (a consequence of deformation) in the upper mantle beneath a seismic station. Here we present SKS splitting measurements from the AK permanent broadband network in Alaska and interpret the results in terms of mantle flow processes.

As a shear wave travels through an anisotropic medium, it is split into orthogonally polarized components aligned with the fast and slow axes of propagation, a phenomenon known as shear wave birefringence or splitting. The orientation and time delay of the component pulses at the receiver reflect the geometry, strength, and extent of anisotropy along the entire ray path. SKS phases are often used in shear wave splitting studies because the P-to-S conversion at the core–mantle boundary controls the initial polarization of the wave before it undergoes splitting in the mantle on the receiver side. Because any contribution to SKS splitting from the lower mantle is generally thought to be small (e.g., Meade et al., 1995; Niu and Perez, 2004), splitting parameters measured from SKS waves are often assumed to reflect anisotropy within the upper mantle and (perhaps) the crust.

The primary mineral phase in the upper mantle is olivine, $(Mg,Fe)_2SiO_4$, which has a single-crystal shear anisotropy of ~18% at upper mantle conditions (e.g., Mainprice, 2007). When an aggregate of olivine undergoes shear deformation in the dislocation creep regime, it develops a lattice-preferred orientation (LPO) and becomes anisotropic on length scales relevant for seismic wave propagation.

---

* Corresponding author at: Department of Geology and Geophysics, Yale University, PO Box 208109, New Haven, CT 06520, USA. Tel.: +1 203 432 5031; fax: +1 203 432 3134.
E-mail address: maureen.long@yale.edu (M.D. Long).

For most temperature, pressure, stress, and volatile content conditions relevant to the upper mantle, the fast axis of shear wave propagation is generally parallel to the direction of maximum shear (e.g., Karato et al., 2008; Zhang and Karato, 1995). For the simple case of horizontal mantle flow with a vertical gradient in flow velocity, the fast shear wave propagation direction thus generally corresponds to the direction of mantle flow beneath a seismic station. There are, however, many possible complications to this simple relationship. In the presence of partial melt, aligned melt pockets can produce shape-preferred orientation (SPO), producing anisotropy that may not be directly related to the flow field (e.g., Zimmerman et al., 1999). Another possible complication is so-called B-type olivine fabric (Jung and Karato, 2001), which changes by 90° the relationship between strain and the resulting anisotropy. This fabric likely predominates in relatively cold conditions with high shear stresses and significant water content (Jung et al., 2006; Karato et al., 2008), which may be found in the shallow corner of the mantle wedge in subduction settings (Kneller et al., 2005, 2008). In addition to complications from melt and B-type olivine fabric, complex anisotropic structures such as multiple and/or dipping layers of anisotropy will influence the splitting patterns at individual stations, causing variations in apparent splitting with backazimuth for SKS phases (e.g., Chevrot and van der Hilst, 2003; Silver and Long, 2011; Silver and Savage, 1994). All these issues demand that caution be exercised when interpreting splitting patterns in terms of physical processes in the upper mantle, particularly in subduction zones.

Alaska is a complex tectonic region. The south-central margin of Alaska exhibits concave curvature toward the subducting Pacific plate, meaning that subduction changes along-strike from normal to highly oblique subduction that transitions to a transform fault in the southeast (Fig. 1). Slab morphology is complicated (e.g., Eberhart-Phillips et al., 2006; Kissling and Lahr, 1991), and the edge of the slab likely introduces complexities in the flow field (e.g., Honda, 2009; Jadamec and Billen, 2010; Kincaid and Griffiths, 2003; Peyton et al., 2001; Piromallo et al., 2006). The age of the slab changes significantly along-strike, from approximately 60 Ma to 20 Ma going west to east (Müller et al., 1997); this implies that the physical properties

of the slab (e.g. density and thermal structure) also vary along-strike. The crustal structure of the overriding plate is also very complicated. The far-field backarc region is relatively simple, with ~25 km thick crust, but within about 500 km of the trench, the crust is thicker and laterally variable, averaging 35–45 km (Veenstra et al., 2006). This area exhibits significant compressive crustal stresses, with many thrust events and a strong seismic–interseismic stress cycle (Ali and Freed, 2010). These complications are compounded by continuing postglacial rebound that may impact the stress field in some regions more than others (Larsen et al., 2005). In addition to potentially affecting mantle flow, these upper plate complications may also contribute another source of coherent and probably very complicated anisotropy if "fossil" anisotropy due to past tectonic processes exists in the overriding plate lithosphere (e.g. Silver, 1996).

In spite of the popularity of the shear wave splitting technique, there are few published studies of shear wave splitting in Alaska, in part due to the paucity of seismic stations. The data that have been published suggest varied and complex anisotropy (Christiensen and Abers, 2010; Wiemer et al., 1999; Yang et al., 1995). Splitting measurements from the temporary BEAAR network in south-central Alaska (Christiensen and Abers, 2010) reveal a strong trench-parallel signal in the north, with a distinct and sharp switch to trench-normal south of the Hine's Creek fault. This abrupt transition is surprising in its sharp localization, but perhaps unsurprising in its approximate location. As suggested by Christiensen and Abers (2010), this E–W line marks a boundary where the depth to the slab is shallower than 70 km and the mantle wedge is therefore very small. The line also marks the lateral transition in crustal thickness, where the overriding crust becomes significantly thicker (Veenstra et al., 2006). All these factors potentially contribute to a substantial change in anisotropic structure. While the dense network is ideal for constraining the location of this change in splitting parameters, a more regionally extensive SKS splitting study may help to better constrain the regional variations in anisotropy.

This study aims to shed more light on the overall regional anisotropic signature through examination of SKS splitting at 54 permanent broadband stations from the AK network (Fig. 2). We processed and analyzed SKS arrivals to determine the splitting parameters ϕ (fast splitting orientation) and δt (delay time). We consider both individual SKS measurements (null and non-null) and the backazimuthal patterns
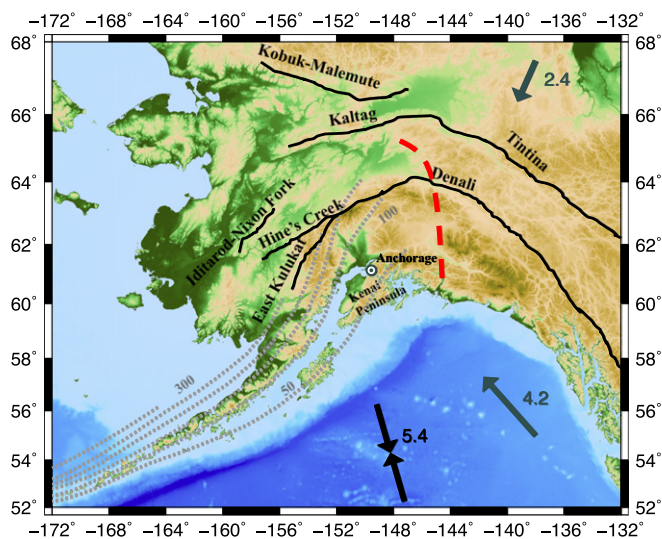
Fig. 1. Tectonic setting of the study region. Major faults are shown in black (Lesh and Ridgway, 2007) along with contours of the subducting slab at 50 km intervals as inferred from seismicity (Gudmundsson and Sambridge, 1998). The absolute motions of the Pacific and North American plates in the NUVEL-1A reference frame (Argus and Gordon, 1991) are shown with gray arrows; the relative motions of the plates are shown with the double black arrows. The dashed red line indicates the approximate location of the edge of the slab at depth (e.g. Jadamec and Billen, 2010).
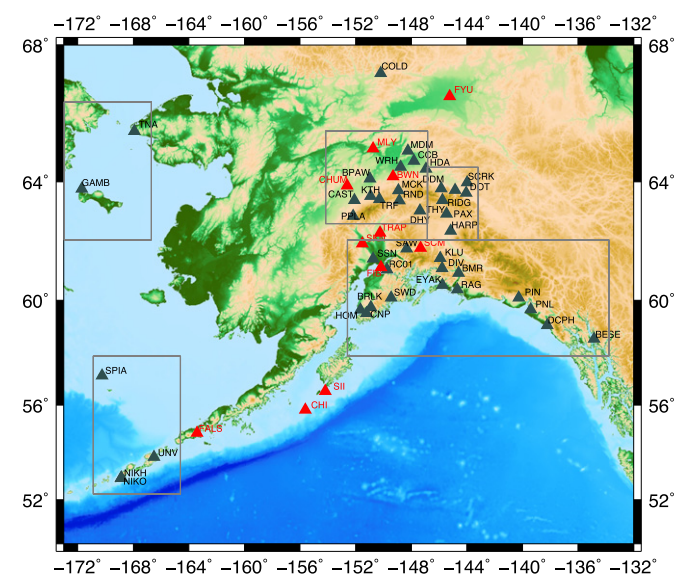
Fig. 2. Map of broadband stations of the AK network used in this study. For stations shown in red, we examined the data but did not identify any high-quality measurements, mainly due to poor data quality and/or a short deployment time. The boxes correspond to the subregions that are shown in Figs. 7–10.
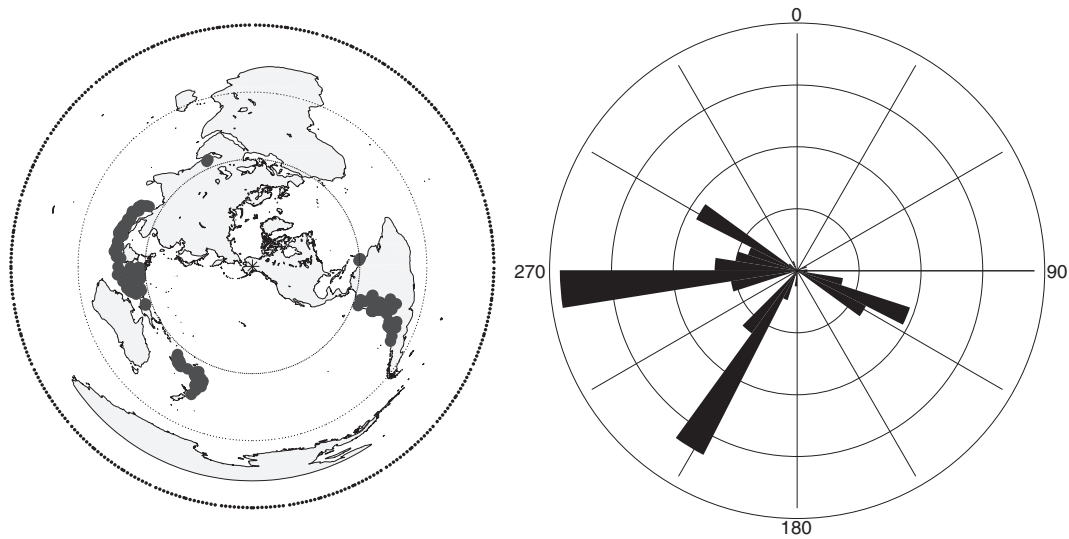
Fig. 3. Event distribution used in this study. a. Map projection of the 242 individual events that yielded at least one useable null or non-null measurement. b. Histogram of back-azimuths for all arrivals in the data set (660 measurements total). Each radial grid line indicates 12 measurements.

of splitting at individual stations. The goal of this work is to examine both the detailed splitting behavior at individual stations and the regional variability in splitting patterns, and to interpret the measurements in terms of subduction-related flow in the upper mantle, which ultimately should shed light on the complex dynamics of the Alaska subduction zone. A broad regional view of shear wave splitting in Alaska is particularly important in light of the planned EarthScope deployment in the region; while the current station coverage is relatively sparse, an understanding of regional-scale splitting patterns will help to frame important unanswered questions relating to mantle dynamics beneath Alaska.

2. Data and methods

### 2.1. Data, preprocessing, and measurement methods

The AK network is a permanent broadband regional network maintained by the Alaska Earthquake Information Center (AEIC) in Fairbanks, Alaska. The stations in the network were deployed over several years, beginning in 1998. The network reaches across mainland Alaska and includes many surrounding islands, but the bulk of the stations are concentrated in the Denali region in south-central Alaska. For this study, all stations with continuous records of more than one year were included, and all data available for each individual station were considered. Because some stations have been running for more than a decade and others are relatively new, the amount of data processed at each station is variable. Thus statistics such as total number of measurements are not entirely meaningful when compared among stations. In all, we measured splitting at 54 different stations, with deployment durations of two to twelve years. Fig. 2 shows a map of all stations included in our study.

We examined SKS arrivals from earthquakes of depth >30 km and magnitude >5.0 at epicentral distances 88°–130° from the station. We examined more than 20,000 unique station-earthquake pairs, producing a total of 660 well-constrained splitting measurements (both null and non-null) from 242 individual earthquakes. The

backazimuthal coverage, shown in Fig. 3, is non uniform, as is typical for SKS splitting studies. We observe SKS arrivals from three distinct directions that correspond to the vast majority of arrivals in our dataset. Fortunately, the spread of arrival directions is sufficient to characterize the anisotropy at most stations. Stations that do not have sufficient backazimuthal coverage to meaningfully constrain splitting parameters individually usually have very few results. These stations are still useful, however, when considered in concert with the rest of the stations in the network. As a whole, the network has reasonably good backazimuthal coverage, leading to confident assessments of splitting parameters, and allowing robust inferences about anisotropic structure.

We preprocessed the data and made splitting measurements using the SplitLab software package (Wüstefeld et al., 2008). We applied a bandpass filter to each waveform, with corner frequencies of 0.01 Hz and either 0.08 Hz, 0.10 Hz or 0.12 Hz, with the cutoff chosen manually (depending on signal and noise properties of each earthquake-station pair) to optimize waveform clarity. A window including at least one period of the SKS arrival at that frequency was manually chosen. We used both the rotation correlation method (e.g., Ando, 1984; Bowman and Ando, 1987; Fukao, 1984), and the transverse component minimization method (Silver and Chan, 1991) to determine splitting parameters. The use of two measurement methods simultaneously helps to ensure that only the highest quality measurements are retained in the data set, since measurement methods can disagree in the presence of noise or for near-null measurements (e.g., Long and Silver, 2009a; Monteiller and Chevrot, 2010; Vecsey et al., 2008; Wustefeld and Bokelmann, 2007). We required that both measurement methods agree for measurements retained in the data set. We only considered events with clear SKS arrivals and a good signal to noise ratio (approximately 3:1 or better) were considered. All waveforms (corrected and uncorrected) and splitting measurement error plots were visually inspected to ensure that SKS arrivals were uncontaminated by other phases and that spitting measurements are well constrained. We manually assigned a quality of "good," "fair," or "poor" to each measurement, based on the signal-to-noise ratio of the

Fig. 4. Examples of typical splitting measurements. The left panels show the uncorrected waveform (dashed line, radial component; solid line, transverse component). The middle panels show the initial (dashed line) and corrected (solid line) particle motion diagrams. The right panel shows the energy map of the transverse component for each possible splitting pair, with the best measurement shown with the crossed lines and the gray ellipse indicating the 95% confidence region. Three examples of split SKS waves are shown in a., b., and c.; an example of a null measurement is shown in d.

a. KTH; 17 Nov 2005   Particle motion before (··) & after (–)   Energy Map of T

b. BESE; 23 April 2004   Particle motion before (··) & after (–)   Energy Map of T

c. BPAW; 21 July 2007   Particle motion before (··) & after (–)   Energy Map of T

d. DOT; 17 Sept 2006   Particle motion before (··) & after (–)   Map of Correlation Coefficient
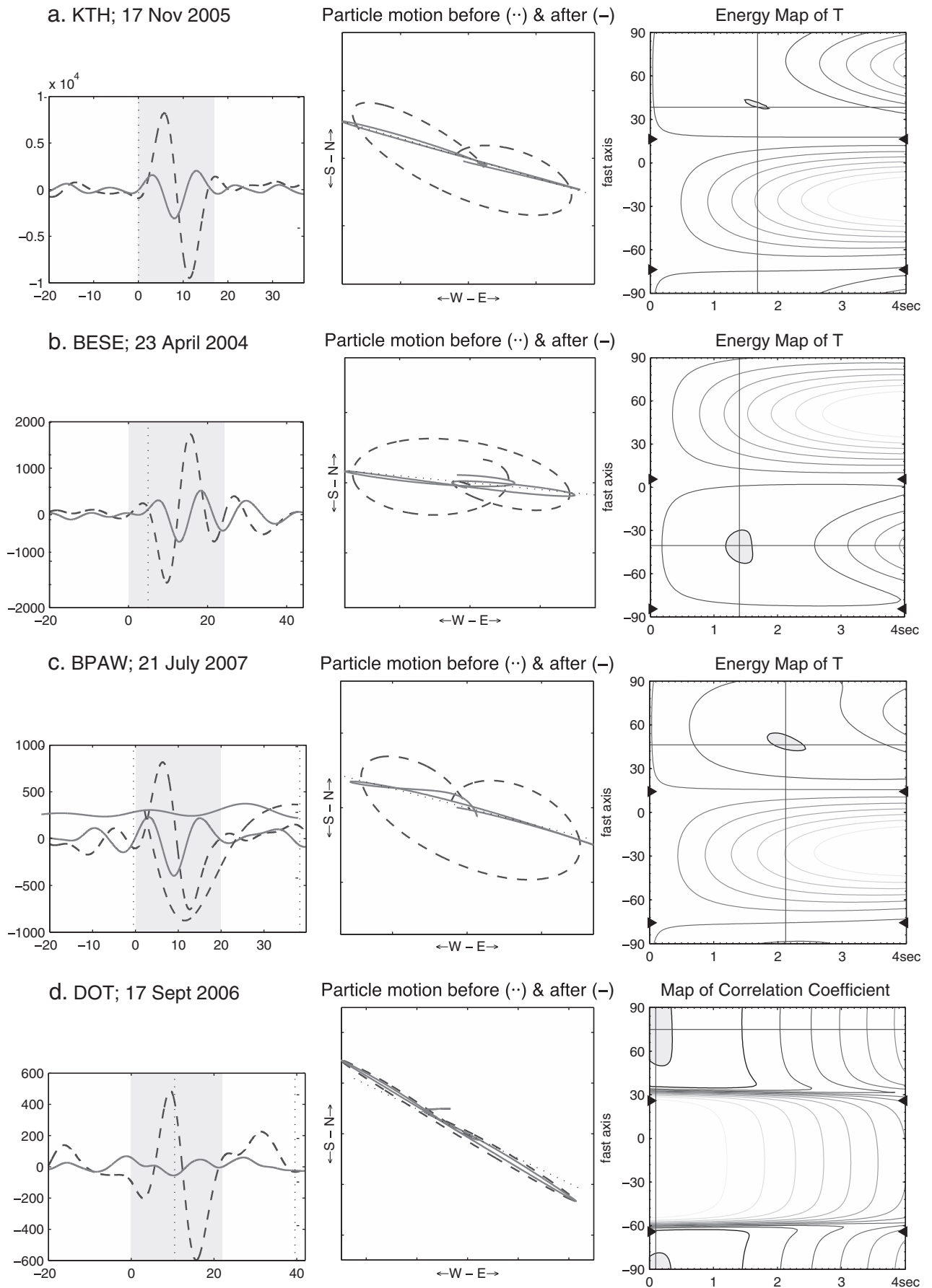
uncorrected and corrected components, the linearity of the corrected particle motion, the size of the error spaces, and how well the best-fitting splitting parameters for each method agreed. For the vast majority of measurements retained in the dataset, 2σ errors are less than ~20°–30° in ϕ and ~0.8–1.0 s in δt. In a very few cases, we retained measurements with 2σ errors as large as 81° in ϕ and 2.9 s in δt, but such measurements were only retained if the two independent measurement methods yielded very similar results; these measurements were characterized as "poor" and were not used in the computation of single-station average splitting parameters. We characterized as null those SKS arrivals that exhibited linear uncorrected particle motion; a null measurement indicates either isotropy or alignment of the backazimuth with the fast or slow axis of the anisotropic medium. Examples of typical measurements, both null and non-null, are shown in Fig. 4.

2.2. Identification of station misalignments

During routine splitting analysis, we identified significant polarization anomalies (that is, differences between the measured initial polarization of the SKS phase and the backazimuth by more than 10°) at many stations, leading to a thorough investigation of possible station misalignments. The AEIC is aware of misalignments at many of the stations in the AK network (Doug Christensen and Roger Hansen, personal communications), including a number of stations aligned to magnetic north rather than true north and a swap of east and north components at station SWD. The magnetic declination in Alaska is more than 20° in some places (Finlay et al., 2010), so stations aligned to magnetic rather than true north are fairly easy to identify. Although there is relatively widespread awareness of alignment problems in the AK network, accurate record of each individual misalignment in the database is incomplete.

Because of the number of misaligned stations and the imperfect knowledge of their true orientations, we carefully considered the possibility of misalignment at each AK station. Station misalignments can be diagnosed through P wave polarization analysis (e.g., Schulte-Pelkum et al., 2001), surface wave polarization analysis (e.g., Ekström and Busby, 2008), or SKS polarization analysis (e.g., Lynner and Long, in press). Here, we estimated station misalignments through polarization analysis of SKS phases, which have been shown to yield estimates of station misalignment that are nearly identical to those obtained through P polarization analysis (Lynner and Long, in press). Initially, we assumed that each station could be misaligned by any amount and used the polarization of split and null measurements and the agreement between the rotation correlation and transverse component minimization measurement methods for split SKS waves to constrain any misalignment. Due to the unmistakable polarization of non-split SKS pulses, the highest-quality nulls were given the most weight when determining appropriate degrees of rotation to correct misalignments. An initial survey of the best-fit station correction for each individual SKS arrival was compiled to find an appropriate correction for each station, and we applied one misalignment value to all events at each station in our subsequent splitting analysis. The station DOT is an exception, having been misaligned when first deployed, but then apparently fixed in November 2008. This change in alignment is reflected in the corrected alignment used for our data processing.

We made a large number of corrections to stations that were not noted as misaligned in the AEIC database. A few appear to be relatively large and seemingly random errors in alignment that cannot be easily explained; however, most corrections were small. Corrections ranged from −68° to +22°. More stations than noted in the database appear to be aligned to magnetic rather than geographic north. The station SWD, for instance, is noted in the database to be rotated 90° from north, but our study suggests that it is misaligned by 68°, likely to magnetic north as well. A complete list of corrected alignments can be found in Appendix A.

Misalignment of stations is an often overlooked but very important factor in shear wave splitting analysis. Evans et al. (2006) show through synthetic seismograms that rotated inputs lead to offsets in ϕ using the rotation correlation method and ϕ and δt using the transverse component minimization method. The different response of the two methods to rotation makes interpretation especially difficult when both methods are used together. As shown in Fig. 5, neglecting to account for station misalignments causes many good arrivals to be categorized as unusable (because results from the measurement methods differ) and will affect calculated splitting parameters for arrivals that are not discarded. The latter is potentially a more significant problem, due to the fact that any physical meaning inferred from the measurements will likely be incorrect. Recently, Tian et al. (2011) published an investigation determining constraints on misalignments of individual stations by comparing the results of different splitting methods assuming a range of station misalignments. Using synthetics as well as real data, they found that the misalignment was correctly determined by the convergence of just a few different splitting methods. They found that the convergence of the transverse component minimization and rotation correlation methods is a good indication of the actual orientation of a station. This suggests that our approach is indeed sufficient to accurately identify station misalignments.

3. Results

3.1. Overall SKS splitting trends for Alaska

Fig. 6 shows all individual split and null measurements, plotted at station locations; individual measurements are also shown in table form in Appendix A. The dominant feature of the splitting parameters in this region is a strong and laterally expansive trench-parallel signal near the middle of Alaska. To the east of this region is a sharp transition to an area of overwhelmingly null measurements. Each of these two regions comprises closely spaced stations with consistent splitting patterns, suggesting strong and coherent anisotropy that is different between the regions. Along the southern coast, the dominant fast directions are approximately trench-normal, but splitting patterns are complicated, with a region around −146° longitude that exhibits many nulls and strong spatial variation in both ϕ and δt. In southeastern Alaska, splitting patterns are simpler, with fast directions that are generally parallel to the coast. Island stations in the Aleutians and off the west coast of Alaska are plagued by poor data quality and sparse coverage, but generally show weak splitting. In all, splitting patterns in Alaska are very complicated, but consistency between proximate stations suggests that these measurements reflect real and meaningful spatial variations in anisotropy.

In order to facilitate the interpretation of our measurements in terms of physical processes, we divide the dataset into separate regions that generally correspond to coherent spatial patterns. We divide the

---

Fig. 5. Examples of splitting measurements at misaligned stations for the case of uncorrected and corrected alignments. Each row shows, from left to right: initial horizontal components of the waveform (solid, N; dashed, E), initial (dashed) and corrected for splitting (solid) particle motions using the transverse component minimization method, and initial (dashed) and corrected for splitting (solid) particle motions using the rotation correlation method. a. Example of a split SKS arrival at station SWD. Top row shows the diagnostic plots uncorrected for misalignment; bottom row shows plots that have been corrected for misalignment. b. Same as a., but for a null measurement at station PAX. Note the disagreement between the methods when the stations are misaligned, and agreement when the misalignment is corrected. The correction at station SWD is −68° and the correction to PAX is +18°.

a. SWD; 25 July 2004
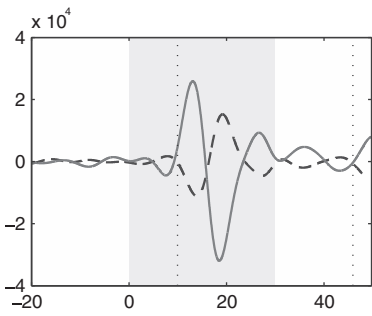
Particle motion before (··) & after (–)
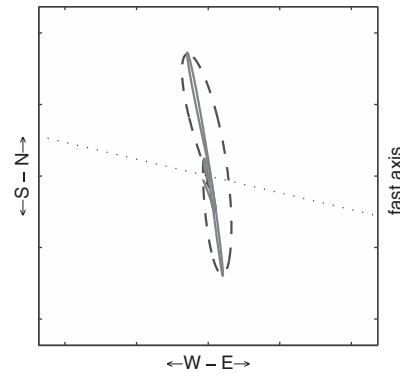
Particle motion before (··) & after (–)
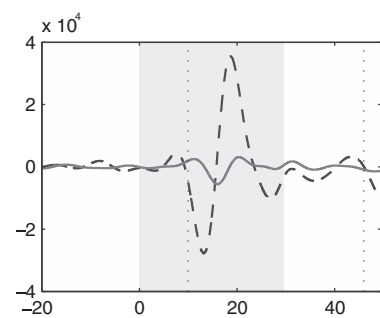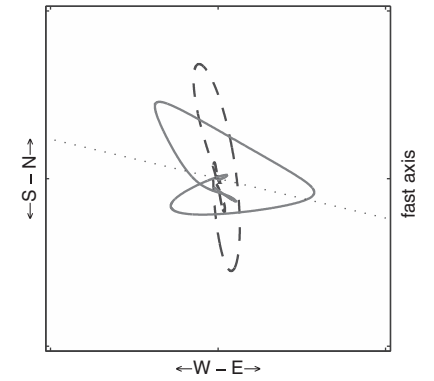
Particle motion before (··) & after (–)
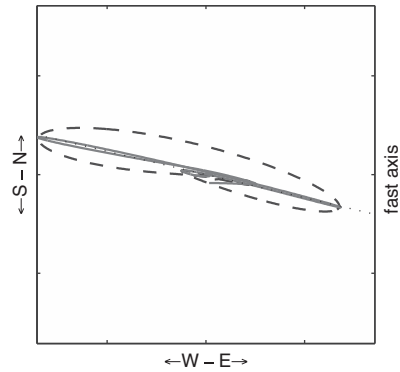
Particle motion before (··) & after (–)
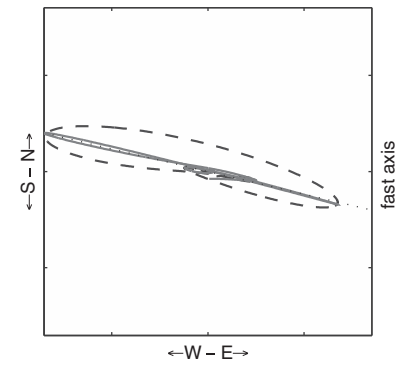
b. PAX; 26 Dec 2004
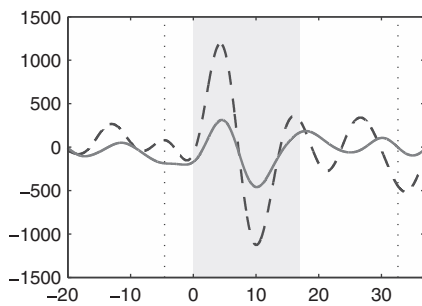
Particle motion before (··) & after (–)
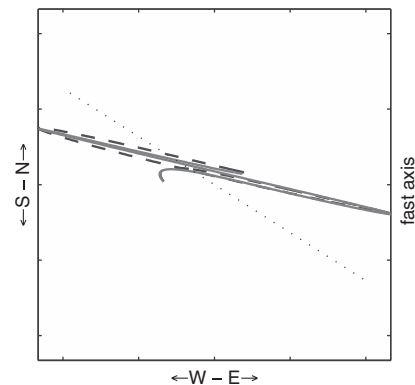
Particle motion before (··) & after (–)
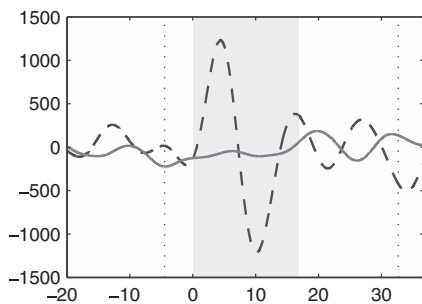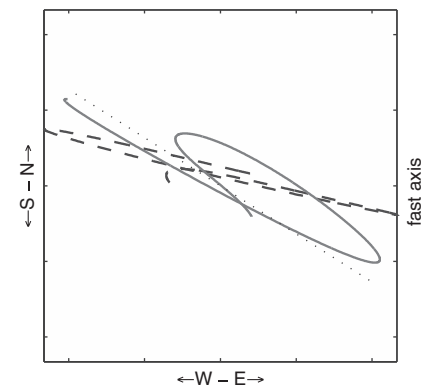
Particle motion before (··) & after (–)
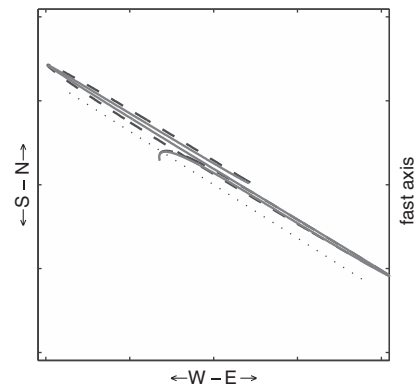
Particle motion before (··) & after (–)
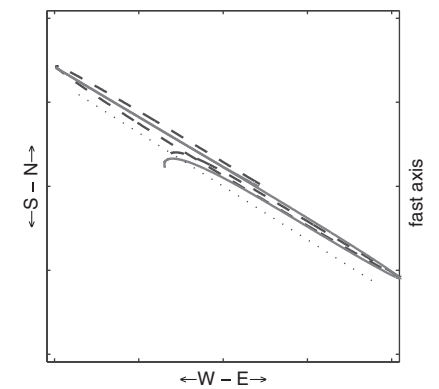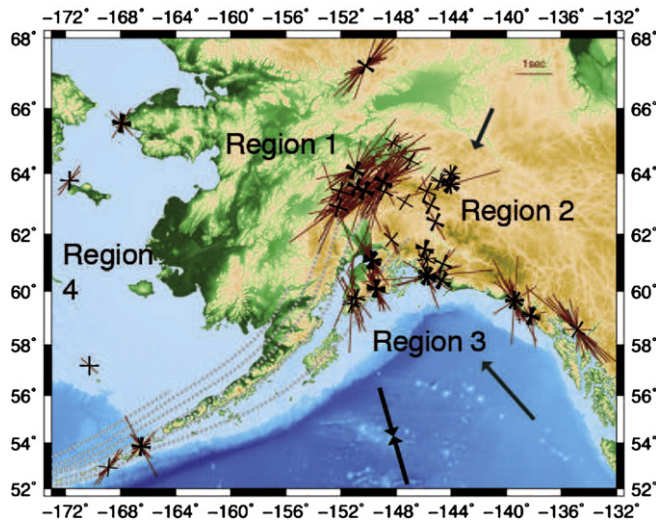
Fig. 6. Map of all individual splitting measurements, both nulls (black crosses) and non-nulls (red bars). Splitting parameters are plotted at the station locations. For non-null splits, the orientation and length of the bar correspond to the fast direction and delay time, respectively. Nulls are plotted as crosses with one arm aligned with the backazimuth and the other aligned orthogonal to it. Symbols indicating plate motions and slab contours are as in Fig. 1.

Fig. 7. Individual splitting measurements for stations in Region 4 (see maps in Figs. 2 and 6). a. Measurements for northwestern Alaska. b. Measurements for the Aleutian arc. Stations are plotted as blue triangles. Splitting measurements are plotted at the 150 km pierce point for each arrival, with null measurements plotted as black crosses and non-null measurements plotted as red bars. Gray arrows indicate the absolute plate motion of the North American plate.

study area into 4 parts (Fig. 6). Region 1, the northernmost section, exhibits strong and fairly consistent splitting parameters with approximately trench parallel fast directions. Region 2, to the southeast of Region 1, exhibits overwhelmingly null splitting patterns. Region 3, along the southern coast of Alaska, is complicated by nulls and a large spread of both ϕ and δt, but suggests a pattern of trench-normal splitting in the direction of Pacific plate motion relative to North America. Region 4 is comprised of mostly island stations in the far west and western Aleutians. Splitting parameters here are not well constrained due to poor data quality and sparse coverage, but show weak splitting (less than 1 s) with predominantly NE–SW fast directions, as well many as null measurements.

3.2. Regional results

Robust analysis of Region 4 is somewhat hampered by poor data quality and sparse coverage. The station distribution here is controlled by the location of islands, and data quality is relatively poor. This means there are fewer usable SKS arrivals than at the quieter inland stations. Some of these stations appear to reflect simple anisotropy, and some reflect very complicated anisotropy (see Fig. 7). TNA and SPIA appear predominantly null, though each also produced some splits. NIKO and NIKH, located less than 4 km from each other, both exhibit stronger splitting (delay times of ~1 s) with a fast axis that is subparallel to the trench. UNV is located less than 200 km northeast of NIKH and NIKO, but exhibits dramatically different splitting. The backazimuthal variations are complex, and the data suggest a complicated anisotropic region. This is in stark contrast to the relatively simple anisotropy suggested by the data at NIKO and NIKH.

Region 1 stations are located such that SKS phases sample the mantle wedge, with the southern edge of the region approximately coincident with the 100 km slab contour (Fig. 6). The fast directions indicated by the splits (Fig. 8) are dominated by NW–SE fast directions and are thus overwhelmingly trench-parallel. The observed null measurements are mostly from events at backazimuths very nearly parallel or perpendicular to the fast axes (Fig. 8). These patterns are consistent with relatively simple anisotropy beneath Region 1 stations.

The stations in Region 2, in sharp contrast to the stations in Region 1, show overwhelmingly null splitting patterns (Fig. 9), with only a few split SKS phases observed. Any single observation of null splitting may be consistent with several scenarios, including isotropic material beneath the station, transverse isotropy with a vertical axis of symmetry, or an initial polarization direction for the SKS phase that is parallel to the fast or slow symmetry axis of the medium. In order to categorize a station or region as truly dominated by nulls and to rule out the third possibility, there must be sufficient backazimuthal coverage to rule out the case in which the fast or slow direction of
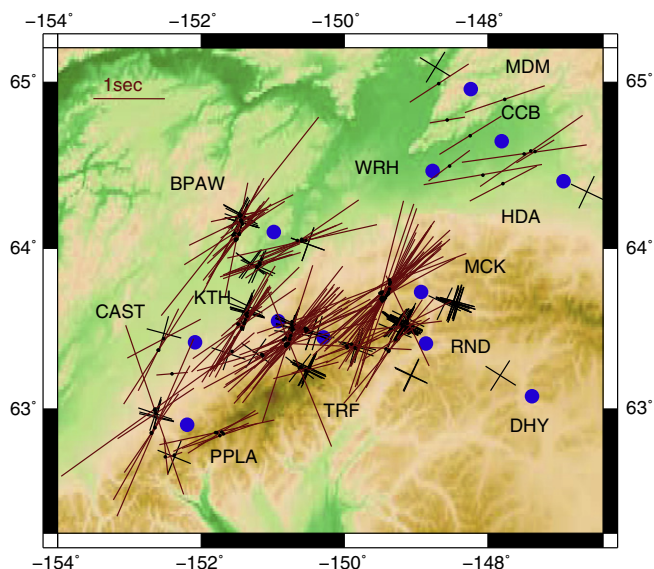
Fig. 8. Individual splitting measurements for stations in Region 1 (see maps in Figs. 2 and 6). Plotting conventions for the measurements and stations are as in Fig. 7.

splitting is coincident with the initial polarization (equivalent to the backazimuth) of the SKS arrival. The backazimuthal coverage for stations in Region 2 is far from ideal (Fig. 9), and at several of the stations the backazimuths of the null measurements coincide with the measured fast directions in Region 1 to the west. However, several of the Region 2 stations do have sufficient backazimuthal coverage to demonstrate that there are null SKS arrivals over a range of back-azimuths. For example, stations SCRK, DOT, and DIV exhibit nulls over several backazimuthal swaths (Fig. 9). This leads us to infer that the predominantly null measurements observed in Region 2 likely reflect "apparent" isotropy in the underlying crust and mantle,
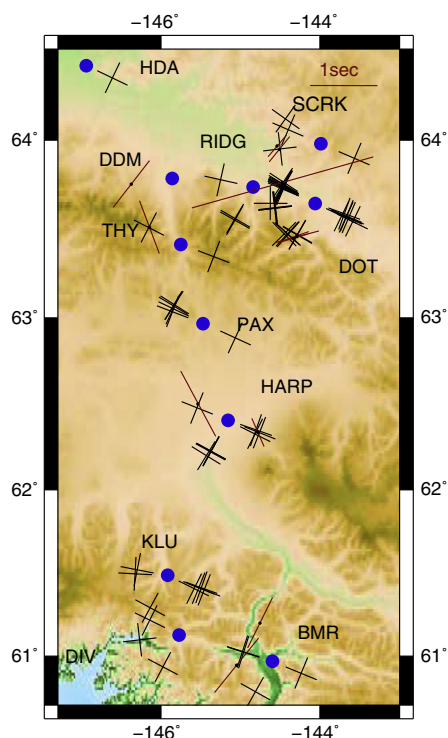
Fig. 9. Individual splitting measurements for stations in Region 2 (see maps in Figs. 2 and 6). Plotting conventions are as in Fig. 7.

which could take the form of true isotropy, transverse isotropy with a vertical axis of symmetry, or small-scale variations in anisotropic structure that appear isotropic to long-wavelength SKS phases.

Region 3 exhibits splitting patterns that are substantially more complicated than the other regions (Fig. 10). Along the southern edge of the Denali block, some stations show strong trench-normal fast directions with varying δt, but other stations exhibit very complicated splitting patterns, with individual measurements varying from null to nearly 3 second delay times (Fig. 10). Most stations in Region 3 exhibit a variety of splitting behavior for different SKS arrivals, with a combination of many split SKS arrivals and many nulls, as well as a mix of different delay times and fast directions. The most extreme complexity is concentrated around the bend in the trench to the east of Anchorage. In the Kanai peninsula, patterns are dominated by generally trench-normal fast directions. Down the coast to the east, in southeast Alaska, splitting patterns are similar to those west of Anchorage. Fast directions here are generally parallel to Pacific plate motion relative to North America (Fig. 10).

There is some evidence for backazimuthal variation in splitting parameters at individual stations, especially near the border between Regions 1 and 2. An example for station MCK is shown in Fig. 11. Arrivals at MCK from the west exhibit splitting behavior similar to that observed most stations in Region 1, whereas arrivals from the east are all null, similar to Region 2, and arrivals from the southwest are mostly null with a few non-null measurements. Station MCK is well placed to record the differing anisotropic properties of the regions, since it is located close to the border between them. Conversely, we do not observe a coherent pattern of backazimuthal variations at most stations; although the backazimuthal coverage at most stations in our study is limited, the observations that we have tend not to display an obvious coherent pattern of backazimuthal variation. For example, station EYAK (Fig. 11) exhibits complicated splitting parameters, but individual measurements appear to vary randomly with backazimuth. This suggests that EYAK overlies laterally contiguous, but complicated anisotropy. The complicated splitting parameters in Region 3 are probably not caused by adjacent regions of simple anisotropy; instead, it is likely that multiple layers or complicated heterogeneities extend over a relatively wide region below the trench.

4. Discussion

4.1. Evaluating possible contributions to SKS splitting

Alaska is a highly complex tectonic setting, with many possible factors contributing to the aggregate anisotropic signal. In addition to flow and deformation in the mantle wedge and sub-slab mantle, there may be a contribution from anisotropy within the slab itself and from the overriding plate lithosphere. Multiple layers of anisotropy, some of which may be dipping, are likely present here, as in most subduction zones. Shear wave splitting studies in subduction settings often ignore contributions from the slab and crust; however, in Alaska it requires closer consideration. The slab morphology is complicated (Eberhart-Phillips et al., 2006; Kissling and Lahr, 1991), so anisotropy within the slab, such as from aligned serpentinized cracks (Faccenda et al., 2008), would result in laterally homogeneous splitting patterns. Because slab morphology may affect mantle flow (e.g., Kneller and van Keken, 2007), the complex slab morphology likely also complicates the resulting anisotropy. The presence of a slab edge is also likely important in this region; flow around this edge may complicate what might otherwise be a simple flow pattern in both the wedge and the sub-slab mantle. Dipping layers of anisotropy are very likely present in any subduction zone; while a dipping axis of anisotropic symmetry will cause complexities in splitting patterns, the dip of the layer is difficult to resolve with splitting measurements alone (Chevrot and van der Hilst, 2003). The physical
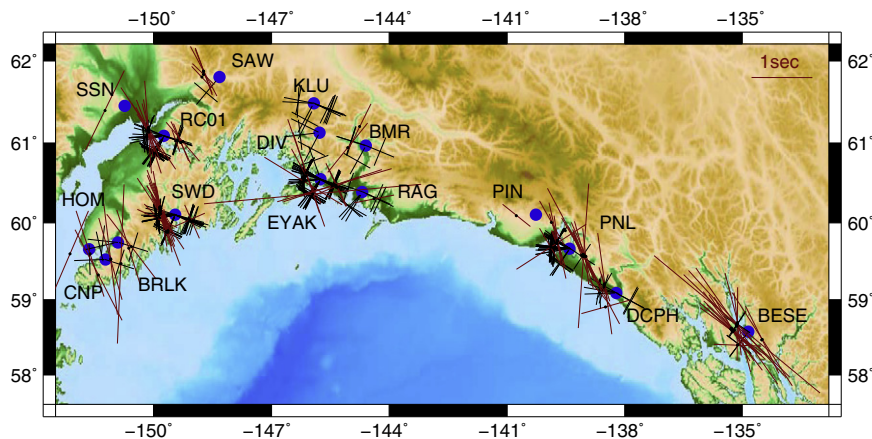
Fig. 10. Individual splitting measurements for stations in Region 3 (see maps in Figs. 2 and 6). Plotting conventions are as in Fig. 7.

interpretation of splitting measurements in a subduction setting must therefore be done with care.

A single SKS splitting measurement cannot be used to constrain the depth of anisotropy, since it represents the integration of the effect of anisotropy along the ray path. However, combining shear wave splitting measurements with other types of seismological data and making some basic physical assumptions can provide a basis for interpreting anisotropy in terms of physical processes. For example, splitting parameters at stations overlying the wedge will likely reflect a contribution from anisotropy due to flow in the mantle wedge, whereas stations located closer to the trench will not. Considering how the spitting signal changes with distance from the trench can give insight into the contribution to splitting from anisotropy in the wedge (e.g., Christiensen and Abers, 2010). Splitting signals from stations relatively far from the trench can give insight to the contribution from mantle flow driven by the motion of the overriding plate.

We can also consider the possibility of contributions to SKS splitting anisotropy in the crust. SKS splitting is nearly always interpreted in terms of mantle anisotropy (e.g., Long and Silver, 2009a, and references therein), but particularly in a region such as Alaska with a crust that is relatively thick (Veenstra et al., 2006) and highly deformed and faulted by past and ongoing deformation (e.g., Ali and Freed, 2010; Cohen and Freymueller, 2004; Ratchkovski and Hansen, 2002), possible contributions from the crust must be considered. The only direct observational constraints on splitting due to crustal anisotropy in Alaska come from the work of Wiemer et al. (1999); the splitting delay times of 0.05–0.1 s for earthquakes at crustal depths ($z = 20$–40 km) as they are observed are much smaller than the SKS delay times documented in this study. Other constraints on Alaskan crustal anisotropy come from a reflection/refraction study by Brocher et al. (1989) and a corresponding laboratory study of crustal anisotropy of rocks from the Valdez Group by Brocher and Christensen (1990). These studies suggest that while crustal P wave anisotropy is likely to be locally strong (~5–9%), the S wave splitting delay times associated with this anisotropy would likely be small. Therefore, while we cannot completely rule out a contribution to our SKS splitting measurements from the crust, we do not believe that it makes the primary contribution to our data set.

Another argument about the most likely depth distribution of anisotropy can also be made on the basis of the lateral variations in splitting patterns. For example, the results from station MCK (discussed above and shown in Fig. 11) offer a line of argument that the differences in splitting patterns between Region 1 and Region 2 reflect relatively deep lateral differences in anisotropy at depth, since SKS phases arriving at MCK from the west seem to sample the relatively simple anisotropic structure beneath Region 1 and SKS phases arriving from the south and east exhibit the predominantly null splitting that

dominates Region 2. We attempt to constrain the depth of anisotropy that causes these variations by calculating Fresnel zones for different arrivals at this same station (e.g., Alsina and Snieder, 1995). At very shallow depths the first Fresnel zones for frequencies relevant to SKS energy (characteristic periods of ~8–10 s) at station MCK would overlap significantly; for example, at a depth of 50 km, the first Fresnel zone for an SKS arrival is ~80 km wide (e.g., Favier and Chevrot, 2003). In general, this would tend to rule out very shallow structure as the source of the observed strong backazimuthal differences (e.g., Alsina and Snieder, 1995), and the largest contribution to the observed splitting likely comes from the asthenospheric mantle rather than the crust and lithospheric mantle.

4.2. Geodynamic interpretation of SKS splitting for different regions

In order to identify the most salient first-order features of our SKS splitting data set, we have computed single-station average splitting parameters for stations where the splitting patterns are simple enough that an average is physically meaningful, and plotted them on a map (Fig. 12) along with the null measurements at Region 2 stations. One of the most striking features of this map is the overwhelming preponderance of dominantly null stations in Region 2. This "apparent" isotropy could be consistent with any one of several different scenarios: the mantle underlying Region 2 may be actually isotropic, it may be anisotropic but includes small-scale heterogeneity (lateral or vertical) that appears isotropic over large length scales, or it may be anisotropic with a vertical axis of symmetry (that is, vertical transverse isotropy or VTI).

Any scenario that invokes anisotropic heterogeneity to explain a region of null measurements requires destructive interference of two or more layers or regions of anisotropy. Complicated flow in the vicinity of the edge of the subducting slab that varies over short length scales may create heterogeneities that cause the region to appear isotropic. A second possibility is that the striking transition in splitting from NW–SE fast directions in Region 1 to predominantly null splitting in Region 2 actually reflects a significant anisotropic domain boundary in the overriding lithosphere, either in the crust, the lithospheric mantle, or perhaps both. Given the location of Region 2 directly above the inferred edge of the subducting slab, we believe that it is more likely that mantle flow near the edge of the slab is the strongest contributing factor in the abrupt change in anisotropy, rather than a transition in lithospheric structure. Also, given the arguments above about the likely small contributions to SKS splitting from the crust, and the arguments based on Fresnel zone analysis for a primary contribution from asthenospheric depths, it is most likely that this transition reflects a change in mantle flow. We emphasize, however, that the data do not completely rule out a contribution from the crust or lithospheric mantle.
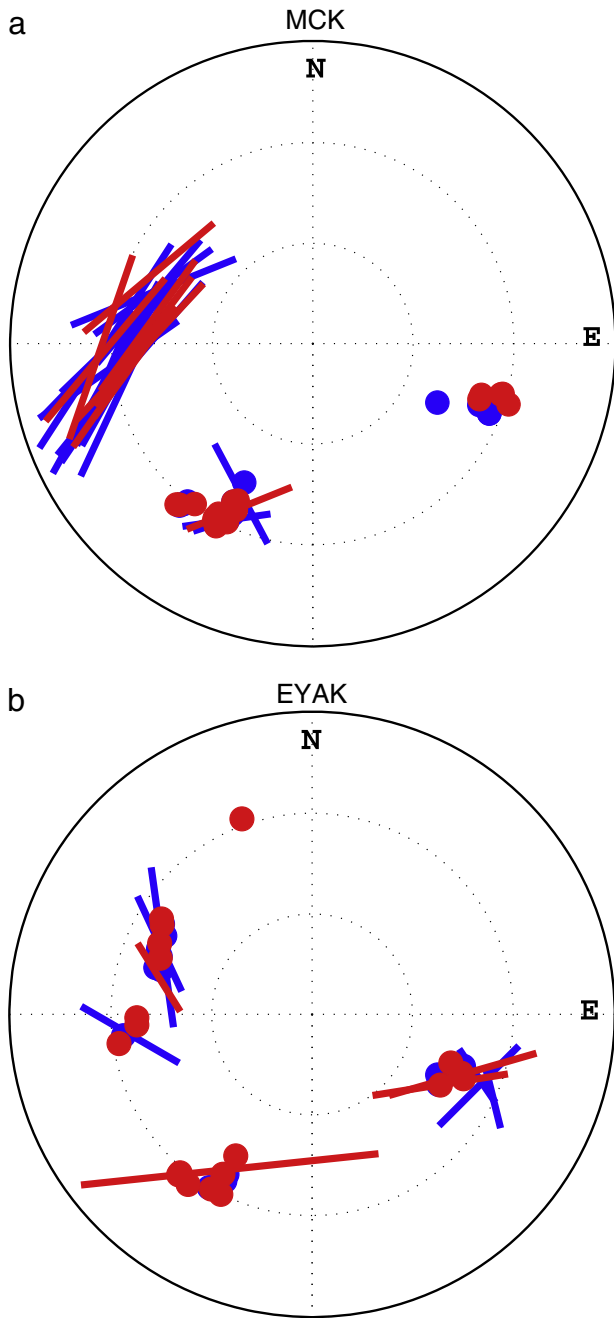
Fig. 11. Stereoplots of splitting patterns at stations MCK (a.) and EYAK (b.). Each measurement is plotted at the location corresponding to the event backazimuth and incidence angle. Bars indicate non-null measurements and dots indicate nulls. Measurements are color-coded by quality, with "good" quality measurements shown in red and "fair" quality measurements shown in blue. "Poor" quality measurements are not shown.

unusual volcanism at Mt. Etna near the Ionian slab (Schellart, 2010). This represents an intriguing possible explanation for our observation, particularly in light of the proximity of Region 2 stations to the Wrangell Volcanic Field.

We do note that shear wave splitting studies in the vicinity of other slab edges (e.g., Eakin et al., 2010; Peyton et al., 2001) have found strong splitting near the edge rather than a region of predominantly null splitting. The study of Peyton et al. (2001) argued for toroidal flow around the edge of the Kamchatka slab, while the dataset of Eakin et al. (2010) in the vicinity of the Mendocino Triple Junction found support for a local perturbation in mantle flow near the southern edge of the Juan de Fuca slab. Both of these studies identified relatively strong splitting in the vicinity of slab edges; the region of null splitting that we observe near the edge of the Alaska slab thus appears to be somewhat unusual when compared to other regions.

Because SKS phases measured at stations in Region 1 sample a large volume of mantle wedge material, we infer that these stations likely reflect trench-parallel anisotropy in the mantle wedge. The strong trench-parallel signal extends south to the location where the depth to the top of the slab is approximately 100 km, and the overriding crust thickens from ~26 km to as much as 45 km (Veenstra et al., 2006). The thicker crust appears to have little effect on the splitting parameters, however. The observed trench-parallel fast directions are most likely due to trench-parallel flow in the mantle wedge, as suggested by Christiensen and Abers (2010), as B-type olivine fabric is not expected in the backarc part of the wedge (Kneller et al., 2005, 2008).

SKS phases measured at stations in Region 3 sample little or none of the mantle wedge, so the observed anisotropy likely reflects flow beneath the Pacific plate, since the wedge is very small or nonexistent beneath these station locations. The middle part of Region 3 is directly
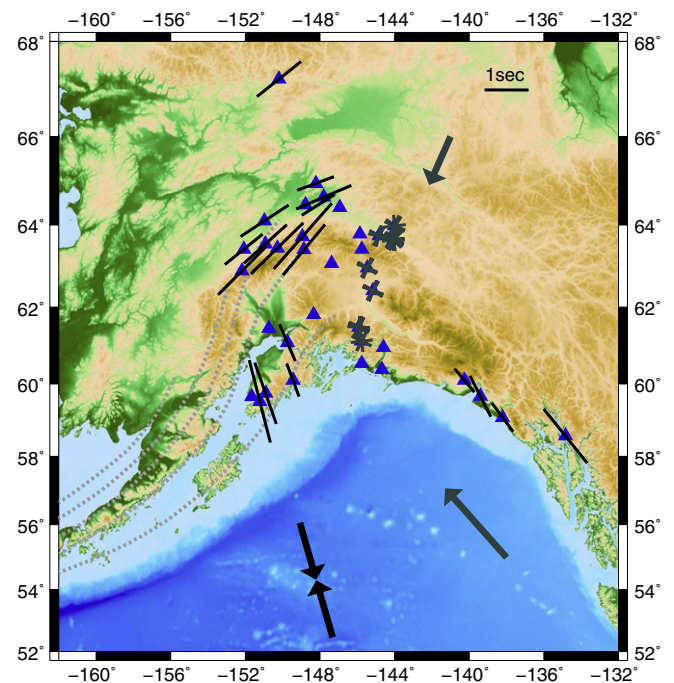

Fig. 12. Map of single-station average splitting parameters (black bars) for those stations where patterns are relatively simple and physically meaningful averages could be obtained (no measurement is shown at stations where this is not the case). Values were obtained by taking a simple (non-weighted) average of all "good" and "fair" quality measurements. For Region 3 stations that are overwhelmingly dominated by nulls, individual null measurements are shown with gray crosses (the few non-null measurements at these stations are not shown). Black arrows indicate the relative plate motion.

One possible scenario for the effect of the slab edge on mantle flow is that there is a strong change in the flow field here due to slab morphology changes, and the apparent isotropy reflects a lack of coherent fabric in the mantle as the regional flow field reorganizes in response to the slab edge. A second, related, possible scenario is that the null splitting reflects anisotropy with a vertical axis of symmetry that is a consequence of predominantly vertical mantle flow at the edge of the slab. Vertical mantle flow at a slab edge has been proposed in other subduction systems (e.g., Civello and Margheriti, 2004), and mantle upwelling has been posited as an explanation for

south of Region 2 (Fig. 2), and shows a large amount of complexity, with complicated backazimuthal dependence of splitting parameters. There are many null measurements, as well as many split SKS arrivals with different fast directions and delay times. There is no simple model that can explain these complex splitting patterns, but we suggest that the most likely explanation is a combination of anisotropy from sub-slab mantle flow, frozen anisotropy in the subducting slab, and perhaps a contribution from frozen anisotropy in the overriding plate as well. While contributions from lithospheric anisotropy in either the slab or the overriding plate may be needed to explain the complex splitting patterns, we do not have an obvious explanation for why this particular part of Region 3 shows more complexity in splitting than other surrounding regions. Fast directions in both the eastern (southeast Alaska), and the western (west of Anchorage) parts of Region 3 are predominantly parallel to Pacific plate motion relative to North America. Upper mantle deformation induced by the relative motion of the Pacific and North American plates is a likely source of the recorded anisotropy. For Region 3 stations located to west of Anchorage, SKS phases have long path lengths in the sub-slab mantle, and a large contribution to the subduction-parallel fast directions from entrained flow beneath the subducting slab is likely. It is worth noting that if this interpretation is correct, then the Alaska subduction zone exhibits different sub-slab mantle flows than most subduction zones worldwide, which tend to be dominated by trench-parallel fast directions (and thus perhaps trench-parallel sub-slab flow) (e.g., Long and Silver, 2009b). The trench-perpendicular fast directions observed at Region 3 stations near the trench also contrast with the roughly trench-parallel fast directions observed at stations NIKO and NIKH further to the west (Fig. 7).

4.3. Comparisons with previous studies

A comparison between our measurements and previously published shear wave splitting data in Alaska is instructive. The splitting patterns in Christensen and Abers (Fig. 13) suggest a strong trench parallel fast axis in the northern part of the BEAAR array and a trench perpendicular fast axis closer to the trench. Christiensen and Abers (2010) interpret this pattern as being due to along-strike flow in

the mantle wedge, and two-dimensional entrained flow below the slab. They observe a sharp change in the fast axis that corresponds approximately with the 70 km slab contour. In regions where the slab is shallower than 70 km, Christiensen and Abers (2010) argue that the wedge is too narrow to contribute significantly to the anisotropy; therefore, the trench-parallel fast directions to the north are most likely due to along-strike flow in the mantle wedge (Christiensen and Abers, 2010). Our data are generally consistent with this scenario, but our dataset covers a wider region (and shows more complexity at individual stations) than was evident from the BEAAR network data.

A recent geodynamical modeling study by Jadamec and Billen (2010) created a three-dimensional numerical model of buoyancy-driven deformation in the Alaska subduction zone. They employed a realistic slab geometry and compared their results with the splitting data from the BEAAR network presented in Christiensen and Abers (2010). Their models emphasized the importance of toroidal flow around the edge of the slab, which in turn is expected to produce complex anisotropic patterns (Jadamec and Billen, 2010). Our observed splitting parameters in Regions 1 and 3 are generally consistent with the predictions of the Jadamec and Billen model, but are also consistent with the hypothesis of Christiensen and Abers (2010) of trench-parallel flow in the mantle wedge and trench-perpendicular flow beneath the slab. We do note that although the predominantly NW–SE fast directions we observe at Region 1 stations are generally consistent with mantle flow around the edge of the slab, as predicted by Jadamec and Billen (2010), this model does not make an explicit prediction of predominantly null measurements right at the slab edge, as we observe in our data. This observation may require a smaller-scale perturbation to the regional flow field, a contribution
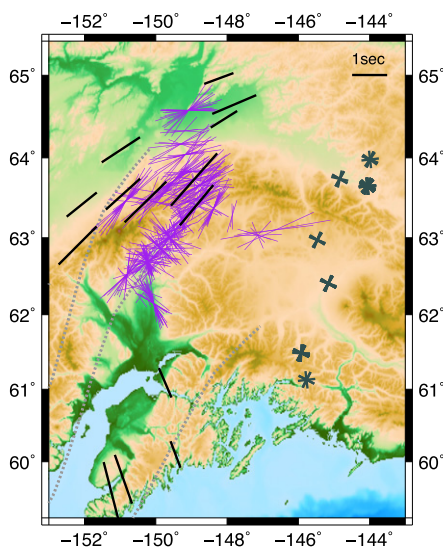
Fig. 13. Comparison between results obtained in this study (black bars and gray crosses, see Fig. 12) and those obtained for stations of the BEAAR array (Christiensen and Abers, 2010). Individual non-null BEAAR measurements are shown with purple bars.
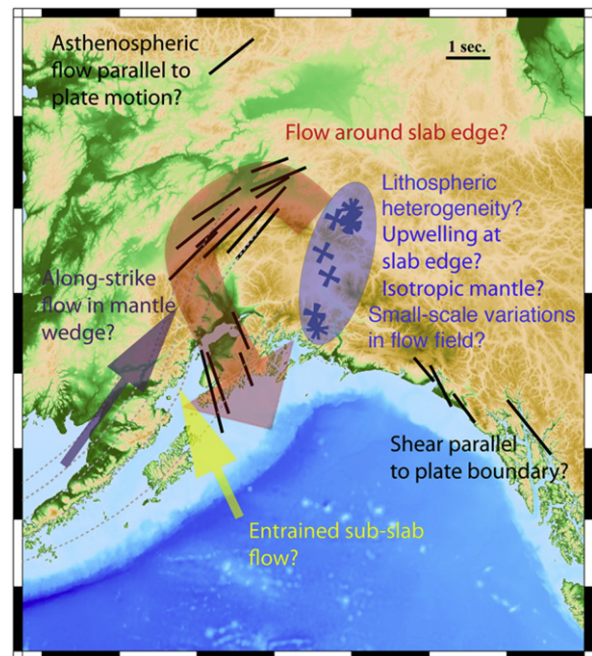
Fig. 14. Cartoon sketch of some physical processes that may be contributing to the upper mantle anisotropy reflected in our SKS splitting dataset. These include shear in the asthenosphere driven by absolute plate motion in the northern part of the study area, along-strike flow in the mantle wedge as suggested by Christiensen and Abers (2010), and plate-boundary-parallel shear in the southeastern part of the study area. The red arrow indicates the rapid mantle flow around the slab edge suggested by Jadamec and Billen (2010). The area dominated by null measurements at the edge of the slab may be a result of lithospheric anisotropic heterogeneity, mantle upwelling at the slab edge, isotropic mantle, a lack of coherent mantle flow resulting from small-scale disturbances in the mantle flow field due to the slab edge, or a combination of these processes.

from heterogeneous anisotropy in the overriding plate lithosphere, or both.

It is also useful to consider comparisons between our measurements and shear wave splitting studies in other subduction zones. As mentioned above, the trench-perpendicular fast directions that we observe in south-central Alaska at stations close to the trench, which mainly sample the mantle beneath the slab, are fairly unusual in the global dataset of subduction zone splitting measurements (e.g., Long and Silver, 2009b) and contrast with measurements at Aleutian stations NIKO and NIKH, which exhibit fast directions that are nearly trench-parallel. Comparisons with other subduction systems where possible mantle flow around slab edges has been suggested is also instructive; the similarities (and differences) between our measurements and data sets from the Kamchatka and Juan de Fuca subduction systems were discussed above. Another useful analog to the Alaskan slab edge may be Italy, where several studies have provided extensive documentation of SKS fast directions that are consistent with toroidal flow beneath the subducting Calabrian slab (e.g., Baccheschi et al., 2008; Civello and Margheriti, 2004; Lucente and Margheriti, 2008), and there may be flow around the slab edge in this region as well. In particular, Lucente and Margheriti (2008) suggested that an area of low splitting delay times may correspond to a region of predominantly vertical flow associated with the fragmentation of the slab at depth, a model that is somewhat similar to the possibility of vertical flow associated with the region of null splitting that we explore here. It is worth noting, however, that the sub-slab fast directions observed in Italy are dominantly trench-parallel, which contrasts with the trench-perpendicular fast directions we document in south-central Alaska.

4.4. Our preferred model for mantle flow beneath Alaska

A schematic cartoon indicating some of the possible contributions to the observed SKS splitting patterns is shown in Fig. 14, and here we summarize our preferred model for anisotropy and mantle flow beneath our study region. Our preferred explanation for the trench-parallel splitting observed in Region 1 is that it is due to trench-parallel flow in the mantle wedge, driven by toroidal flow around the slab edge (Jadamec and Billen, 2010), by the complex slab morphology (Kneller and van Keken, 2007), or by some other mechanism. The predominantly null region we observe in Region 2 is most likely due to either complex, small-scale variations in mantle flow that give rise to very small-scale anisotropic heterogeneity or to predominantly vertical flow which results in a vertical axis of anisotropic symmetry. An intriguing possibility is that there is a localized mantle upwelling at the edge of the Alaska slab, as has been suggested for other regions (e.g., Schellart, 2010), but the data do not allow us to distinguish among the several possibilities. In any case, the distinctive splitting pattern in Region 2 most likely reflects the effect of the slab edge on the mantle flow field. Region 3 stations located directly to the south of Region 1 likely reflect a primary contribution from entrained flow beneath the downgoing slab, while stations in the southeast part of the AK array located near the Pacific–North American transform boundary likely reflect plate-boundary-parallel shearing in the upper mantle. The northernmost station shown in Fig. 14 has a fast direction parallel to the absolute plate motion of the North American plate, and likely reflects shear in the asthenospheric mantle due to this plate motion.

4.5. Looking ahead to USArray in Alaska

Unfortunately, the SKS splitting data set presented here is insufficient to distinguish among the possible models for mantle flow beneath Alaska. Our data do indicate that the dynamics of this region are much more complicated than the classical model of two-dimensional corner flow, and that this region warrants further

study. The USArray Transportable Array, part of the EarthScope project (www.earthscope.org), is slated for deployment in Alaska starting in ~2014 and we expect that the spatially dense data set from the Alaska TA stations will shed light on the details of the complex anisotropic structure suggested by our observations. Given the predominantly null splitting that we observed at stations that overlie the slab edge, it is particularly important that future studies of SKS splitting using TA data in Alaska pay careful attention to the delineation and interpretation of null SKS measurements. Seismological observations that place constraints on the depth distribution of anisotropy (such as surface wave dispersion or anisotropic receiver function analysis) will be an invaluable complement to SKS splitting data sets, and the combination of different types of seismological analyses to constrain depth-dependent seismic anisotropy should be a high priority for studies using Alaska TA data.

5. Summary

We examined more than 20,000 SKS waveforms measured at stations of the AK network and measured shear wave splitting parameters (ϕ and δt) in order to study mantle flow in the Alaska subduction system. In the northern part of the array, observed fast splitting directions are overwhelmingly trench parallel, and splitting patterns at individual stations are remarkably consistent. To the east of the Denali block, at stations that roughly overlie the edge of the subducting slab at depth, there is a region dominated by null measurements. The transition from strongly trench parallel to null is sharp and can even be seen at some stations (e.g. MCK) in the backazimuthal variation of splitting measurements. South of the null region is a small region of extremely complicated splitting measurements that also exhibit complicated backazimuthal dependence. To either side of this region along the coast, splitting measurements are predominantly parallel to Pacific plate motion.

Overall the splitting patterns presented in this study are complicated, and could be consistent with several different hypotheses for mantle flow in the vicinity of the slab. While our data set does not uniquely constrain a model for upper mantle flow beneath the study region, our preferred model for the observed splitting patterns can be summarized as follows. Far from the trench in the northernmost part of the study area, plate-motion-parallel shear in the asthenosphere dominates. Closer to the trench, the mantle flow field is predominantly controlled by subduction-related processes. Stations located closest to the trench predominantly reflect flow beneath the subducting slab, which is roughly trench-parallel in the Aleutians with a transition to entrained flow at stations close to the eastern edge of the slab. Predominantly NW–SE fast directions observed in the central part of our study area reflect trench-parallel flow around the slab edge, similar to models proposed by Christiensen and Abers (2010) and Jadamec and Billen (2010). Stations that overlie the slab edge exhibit predominantly null splitting, which is most likely due to small-scale variations in mantle flow associated with the slab edge or to predominantly vertical flow at the slab edge. Stations in the southeastern part of Alaska reflect plate-motion-parallel shear in the upper mantle in the vicinity of the transform plate boundary.

While our dataset appears to reflect a contribution from a number of different physical mechanisms, it is insufficient to uniquely determine the pattern of mantle flow in the mantle wedge, beneath the slab, and in the vicinity of the slab edge. The limited geographical coverage of the AK network represents the most important limitation on our ability to constrain the mantle flow patterns in the Alaska subduction zone. The USArray Transportable Array (TA) is scheduled to deploy in Alaska starting in 2014, and this experiment will provide an excellent opportunity to study this region further and to come to a

more complete understanding of the mantle dynamics of the Alaska subduction zone.

Acknowledgments

Appendix A. Supplementary data

A complete list of station misalignments, individual splitting measurements, average single-station splitting parameters, and stereoplots of single-station splitting patterns can be found in the Appendix. Supplementary data to this article can be found online at doi:10.1016/j.tecto.2012.01.003.

References

Ali, S.T., Freed, A.M., 2010. Contemporary deformation and stressing rates in southern Alaska. Geophysical Journal International 183, 557–571.

Alsina, D., Snieder, R., 1995. Small-scale sublithospheric continental mantle deformation constraints from SKS splitting observations. Geophysical Journal International 123, 431–448.

Ando, M., 1984. ScS polarization anisotropy around the Pacific Ocean. Journal of Physics of the Earth 32, 179–195.

Argus, D.F., Gordon, R.G., 1991. No-net-rotation model of current plate velocities incorporating plate motion model NUVEL-1. Geophysical Research Letters 18, 2039–2042.

Baccheschi, P., Margheriti, L., Steckler, M.S., 2008. SKS splitting in southern Italy: anisotropy variations in a fragmented subduction zone. Tectonophysics 462, 49–67.

Bowman, J.R., Ando, M., 1987. Shear-wave splitting in the upper mantle wedge above the Tonga subduction zone. Geophysical Journal of the Royal Astronomical Society 88, 25–41.

Brocher, T.M., Christensen, N.I., 1990. Seismic anisotropy due to preferred mineral orientation observed in shallow crustal rocks in southern Alaska. Geology 18, 737–740.

Brocher, T.M., Fisher, M.A., Geist, E.L., Christensen, N.I., 1989. A high-resolution seismic reflection/refraction study of the Chugach–Peninsular terrane boundary, southern Alaska. Journal of Geophysical Research 94, 4441–4455.

Chevrot, S., van der Hilst, R.D., 2003. On the effects of a dipping axis of symmetry on shear wave splitting measurements. Geophysical Journal International 152, 497–505.

Christensen, D.H., Abers, G.A., 2010. Seismic anisotropy under central Alaska from SKS splitting observations. Journal of Geophysical Research 115, B04315. doi:10.1029/2009JB006712.

Civello, S., Margheriti, L., 2004. Toroidal mantle flow around the Calabrian slab (Italy) from SKS splitting. Geophysical Research Letters 31, L10601. doi:10.1029/2004GL019607.

Cohen, S.C., Freymueller, J.T., 2004. Crustal deformation in Southcentral Alaska: the 1964 Prince William Sound earthquake subduction zone. Advances in Geophysics 47, 1–63.

Eakin, C.M., Obrebski, M., Allen, R.M., Boyarko, D.C., Brudzinski, M.R., Porritt, R., 2010. Seismic anisotropy beneath Cascadia and the Mendocino triple junction: interaction of the subducting slab with mantle flow. Earth and Planetary Science Letters 297, 627–632.

Eberhart-Phillips, D., Christensen, D.H., Brocher, T.M., Hansen, R., Ruppert, N.A., Haeussler, P.J., Abers, G.A., 2006. Imaging the transition from Aleutian subduction to Yukatat collision in central Alaska, with local earthquakes and active source data. Journal of Geophysical Research 111, B11303. doi:10.1029/2005JB004240.

Ekström, G., Busby, R.W., 2008. Measurements of seismometer orientation at USArray Transportable Array and backbone stations. Seismological Research Letters 79, 554–561.

Evans, M.S., Kendall, J.M., Willemann, R.J., 2006. Automated SKS splitting and upper-mantle anisotropy beneath Canadian seismic stations. Geophysical Journal International 165, 931–942.

Faccenda, M., Burlini, L., Gerya, T.V., Manprice, D., 2008. Fault-induced seismic anisotropy by hydration in subducting oceanic plates. Nature 455, 1097–1101.

Favier, N., Chevrot, S., 2003. Sensitivity kernels for shear wave splitting in transverse isotropic media. Geophysical Journal International 153, 213–228.

Finlay, C.C., et al., 2010. International geomagnetic reference field: the eleventh generation. Geophysical Journal International 183, 1216–1230.

Fukao, Y., 1984. Evidence from core-reflected shear waves for anisotropy in the earth's mantle. Nature 309, 695–698.

Gudmundsson, O., Sambridge, M., 1998. A regionalized upper mantle (RUM) seismic model. Journal of Geophysical Research 103, 7121–7136.

Honda, S., 2009. Numerical simulations of mantle flow around slab edges. Earth and Planetary Science Letters 277, 112–122.

Jadamec, M.A., Billen, M.I., 2010. Reconciling surface plate motions with rapid three dimensional mantle flow around a slab edge. Nature 465, 338–341.

Jung, H., Karato, S., 2001. Water-induced fabric transitions in olivine. Science 293, 1460–1463.

Jung, H., Katayama, I., Jiang, Z., Hiraga, T., Karato, S., 2006. Effect of water and stress on the lattice-preferred orientation of olivine. Tectonophysics 421, 1–22.

Karato, S., Jung, H., Katayama, I., Skemer, P.A., 2008. Geodynamic significance of seismic anisotropy of the upper mantle: new insights from laboratory studies. Annual Review of Earth and Planetary Sciences 36, 59–95.

Kincaid, C., Griffiths, R.W., 2003. Laboratory models of the thermal evolution of the mantle during rollback subduction. Nature 425, 58–62.

Kissling, E., Lahr, J.C., 1991. Tomographic image of the Pacific slab under southern Alaska. Eclogae Geologicae Helvetiae 84, 297–315.

Kneller, E.A., van Keken, P.E., Karato, S., Park, J., 2005. B-type olivine fabric in the mantle wedge: insights from high-resolution non-Newtonian subduction zone models. Earth and Planetary Science Letters 237, 781–797.

Kneller, E.A., van Keken, P.E., 2007. Trench parallel flow and seismic anisotropy in the Marianas and Andean subduction systems. Nature 450, 1222–1225.

Kneller, E.A., Long, M.D., van Keken, P.E., 2008. Olivine fabric transitions and shear wave anisotropy in the Ryukyu subduction system. Earth and Planetary Science Letters 268, 268–282.

Larsen, C.F., Motyka, R.J., Freymueller, J.T., Echelmeyer, K.A., Ivins, E.R., 2005. Rapid viscoelastic uplift in southeast Alaska caused by post-Little Ice Age glacial retreat. Earth and Planetary Science Letters 237, 548–560.

Lesh, M.E., Ridgway, K.D., 2007. Geomorphic evidence of active transpressional deformation in the Tanana foreland basin, south-central Alaska. In: Ridgeway, K.D., et al. (Ed.), Tectonic Growth of a Collisional Continental Margin: Crustal Evolution of Southern Alaska: Geol. Soc. Am. Spec. Pap., 431. doi:10.1120/2007.2431.

Long, M.D., Silver, P.G., 2009a. Shear wave splitting and mantle anisotropy: measurements, interpretations, and new directions. Surveys in Geophysics 30, 407–461.

Long, M.D., Silver, P.G., 2009b. Mantle flow in subduction systems: the subslab flow field and implications for mantle dynamics. Journal of Geophysical Research 114, B10312. doi:10.1029/2008JB006200.

Lucente, F.P., Margheriti, L., 2008. Subduction rollback, slab breakoff, and induced strain in the uppermost mantle beneath Italy. Geology 36, 375–378.

Lynner, C., Long, M.D., in press. Evaluating contributions to SK(K)S splitting from lower mantle anisotropy: a case study from station DBIC, Côte d'Ivoire. Bulletin of the Seismological Society of America.

Mainprice, D., 2007. Seismic anisotropy of the deep Earth from a mineral and rock physics perspective. In: Schubert, G. (Ed.), Treatise On Geophysics, vol. 2. Elsevier, New York, pp. 437–491.

Meade, C., Silver, P.G., Kaneshima, S., 1995. Laboratory and seismological observations of lower mantle anisotropy. Geophysical Research Letters 22, 1293–1296.

Monteiller, V., Chevrot, S., 2010. How to make robust splitting measurements for single-station analysis and three-dimensional imaging of seismic anisotropy. Geophysical Journal International 182, 311–328.

Müller, R.D., Roest, W.R., Royer, J.Y., Gahagan, L.M., Sclater, J.G., 1997. Digital isochrones of the world's ocean floor. Journal of Geophysical Research 102, 3211–3214.

Niu, F., Perez, A.M., 2004. Seismic anisotropy in the lower mantle: a comparison of waveform splitting of SKS and SKKS. Geophysical Research Letters 31, L24612. doi:10.1029/2004GL021196.

Peyton, V., Levin, V., Park, J., Brandon, M., Lees, J., Gordeev, E., Ozerov, A., 2001. Mantle flow at a slab edge: seismic anisotropy in the Kamchatka region. Geophysical Research Letters 28, 379–382.

Piromallo, C., Becker, T.W., Funiciello, F., Faccenna, C., 2006. Three-dimensional instantaneous mantle flow induced by subduction. Geophysical Research Letters 33, L08304. doi:10.1029/2005GL025390.

Ratchkovski, N.A., Hansen, R.A., 2002. New constrains on tectonics of interior Alaska: earthquake locations, source mechanisms and stress regime. Bulletin of the Seismological Society of America 92, 998–1014.

Schellart, W.P., 2010. Mount Etna–Iblean volcanism caused by rollback-induced upper mantle upwelling around the Ionian slab edge: an alternative to the plume model. Geology 38, 691–694.

Schulte-Pelkum, V., Masters, G., Shearer, P.M., 2001. Upper mantle anisotropy from long-period P polarization. Journal of Geophysical Research 106, 21,917–21,934.

Silver, P.G., Chan, W.W., 1991. Shear wave splitting and subcontinental mantle deformation. Journal of Geophysical Research 96, 16429–16454.

Silver, P.G., Savage, M.K., 1994. The interpretation of shear-wave splitting parameters in the presence of two anisotropic layers. Geophysical Journal International 119, 949–963.

Silver, P.G., 1996. Seismic anisotropy beneath the continents: probing the depths of geology. Annual Review of Earth and Planetary Sciences 24, 385–432.

Silver, P.G., Long, M.D., 2011. The non-commutivity of shear wave splitting operators at low frequencies and implications for anisotropy tomography. Geophysical Journal International 184, 1415–1427.

Tian, X., Zhang, J., Si, S., Wang, J., Chen, Y., Zhang, Z., 2011. SKS splitting measurements with horizontal component misalignment. Geophysical Journal International 185, 329–340.

Vecsey, L., Plomerova, J., Babuska, V., 2008. Shear-wave splitting measurements: problems and solutions. Tectonophysics 462, 178–196.

Veenstra, E., Christensen, D.H., Abers, G.A., Ferris, A., 2006. Crustal thickness variation in south-central Alaska. Geology 34, 781–784.

Wiemer, S., Tytgat, G., Wyss, M., Duenkel, U., 1999. Evidence for shear-wave anisotropy in the mantle wedge beneath south-central Alaska. Bulletin of the Seismological Society of America 89, 1313–1322.

Wüstefeld, A., Bokelmann, G.H.R., Zaroli, C., Barruol, G., 2008. Splitlab — a shear wave splitting environment in MatLab. Computers & Geosciences 34, 5515–5528.

Wustefeld, A., Bokelmann, G., 2007. Null detection in shear-wave splitting measurements. Bulletin of the Seismological Society of America 97, 1204–1211.

Yang, X., Fischer, K.M., Abers, G.A., 1995. Seismic anisotropy beneath the Shumagin Islands segment of the Aleutian–Alaska subduction zone. Journal of Geophysical Research 100, 18165–18177.

Zhang, S., Karato, S., 1995. Lattice preferred orientation of olivine aggregates deformed in simple shear. Nature 375, 774–777.

Zimmerman, M.E., Zhang, S., Kohlstedt, D.L., Karato, S., 1999. Melt distribution in mantle rocks deformed in simple shear. Geophysical Research Letters 26, 1505–1508.